arXiv:hep-ph/0005112v1 11 May 2000

Heavy Quark Production and PDF's Subgroup Report*

R. Demina[a], S. Keller[b], M. Krämer[c], S. Kretzer[d], R. Martin[e], F.I. Olness[f,†], R.J. Scalise[f], D.E. Soper[g], W.-K. Tung[h,i], N. Varelas[e], U.K. Yang[j]

[a]Kansas State University, Physics Department, 116 Cardwell Hall, Manhattan, KS 66506
[b]Theoretical Physics Division, CERN, CH-1211 Geneva 23, Switzerland
[c]Department of Physics, University of Edinburgh, Edinburgh EH9 3JZ, Scotland
[d]Univ. Dortmund, Dept. of Physics, D-44227 Dortmund, Germany
[e]Univ. of Illinois at Chicago, Dept. of Physics, Chicago, IL 60607
[f]Southern Methodist University, Department of Physics, Dallas, TX 75275-0175
[g]Institute of Theoretical Science, University of Oregon, Eugene OR 97403, USA
[h]Michigan State University, Department of Physics and Astronomy, East Lansing, Michigan 48824-1116
[i]Fermi National Accelerator Laboratory, Batavia, IL 60510
[j]University of Chicago, Enrico Fermi Institute, Chicago, IL 60637-1434

We present a status report of a variety of projects related to heavy quark production and parton distributions for the Tevatron Run II.

1. Introduction

The production of heavy quarks, both hadroproduction and leptoproduction, has become an important theoretical and phenomenological issue. While the hadroproduction mode is of direct interest to this workshop,[1] we shall find that the simpler leptoproduction process can provide important insights into the fundamental production mechanisms.[2, 3, 4, 5] Therefore, in preparation for the Tevatron Run II, we must consider information from a variety of sources including charm and bottom production at fixed-target and collider lepton and hadron facilities.

For example, the charm contribution to the total structure function F_2 at HERA, is sizeable, up to $\sim 25\%$ in the small x region.[4] Therefore a proper description of charm-quark production is required for a global analysis of structure function data, and hence a precise extraction of the parton densities in the proton. These elements are important for addressing a variety of issues at the Tevatron.

In addition to the studies investigated at the Run II workshop series,[1] we want to call attention to the extensive work done in the *Standard Model Physics (and more) at the LHC Workshop* organized by Guido Altarelli, Daniel Denegri, Daniel Froidevaux, Michelangelo Mangano, Tatsuya Nakada which was held at CERN during the same period.[2] In particular, the investigations of the LHC *b-production group* (convenors: Paolo Nason, Giovanni Ridolfi, Olivier Schneider, Giuseppe Tartarelli, Vikas Pratibha) and the *QCD group* (convenors: Stefano Catani, Davison Soper, W. James Stirling, Stefan Tapprogge, Michael Dittmar) are directly relevant to the material discussed here. Furthermore, our report limits its scope to the issues discussed within the Run II workshop; for a recent comprehensive review, see Ref. [6].

2. Schemes for Heavy Quark Production

Heavy quark production also provides an important theoretical challenge as the presence of the heavy quark mass, M, introduces a new scale into the problem. The heavy quark mass scale, M, in addition to the characteristic energy scale of the process (which we will label here generically as E), will require a different organization of the perturbation series depending on the relative magnitudes of M and E. We find there are essentially two cases to consider.[3]

1. For the case of $E \sim M$, heavy-quark production is calculated in the so-called fixed flavor number (FFN) scheme from hard processes initiated by light quarks (u, d, s) and gluons, where all effects

*Contribution to the Physics at Run II Workshops: QCD and Weak Boson Physics, Fermilab, 1999.
†Sub-group convenor.
[1]In particular, in the Run II B-Physics workshop, the studies of *Working Group 4: Production, Fragmentation, Spectroscopy*, organized by Eric Braaten, Keith Ellis, Eric Laenen, William Trischuk, Rick Van Kooten, and Scott Menary, addressed many issues of direct interest to this subgroup. The report is in progress, and the web page is located at: http://www-theory.fnal.gov/people/ligeti/Brun2/
[2]The main web page is located at: http://home.cern.ch/~mlm/lhc99/lhcworkshop.html
[3]We emphasize that the choice of a prescription for dealing with quark masses in the hard scattering coefficients for deeply inelastic scattering is a separate issue from the choice of definition of the parton distribution functions. For all of the prescriptions discussed here, one uses the standard $\overline{\rm MS}$ definition of parton distributions.

of the charm quark are contained in the perturbative coefficient functions. The FFN scheme incorporates the correct threshold behavior, but for large scales, $E \gg M$, the coefficient functions in the FFN scheme at higher orders in α_s contain potentially large logarithms $\ln^n(E^2/M^2)$, which may need to be resummed.[7, 8, 9, 10]

2. For the case of $E \gg M$, it is necessary to include the heavy quark as an active parton in the proton. This serves to resum the potentially large logarithms $\ln^n(E^2/M^2)$ discussed above. The simplest approach incorporating this idea is the so-called zero mass variable flavor number (ZM-VFN) scheme, where heavy quarks are treated as infinitely massive below some scale $E \sim M$ and massless above this threshold. This prescription has been used in global fits for many years, but it has an error of $\mathcal{O}(M^2/E^2)$ and is not suited for quantitative analyses unless $E \gg M$.

While the extreme limits $E \gg M$ and $E \sim M$ are straightforward, much of the experimental data lie in the intermediate region As such, the correct PQCD formulation of heavy quark production, capable of spanning the full energy range, must incorporate the physics of both the FFN scheme and the ZM-VFN scheme. Considerable effort has been made to devise a prescription for heavy-flavor production that interpolates between the FFN scheme close to threshold and the ZM-VFN scheme at large E.

The generalized VFN scheme includes the heavy quark as an active parton flavor and involves matching between the FFN scheme with three active flavors and a four-flavor prescription with non-zero heavy-quark mass. It employs the fact that the mass singularities associated with the heavy-quark mass can be resummed into the parton distributions without taking the limit $M \to 0$ in the short-distance coefficient functions, as done in the ZM-VFN scheme. This is precisely the underlying idea of the Aivazis–Collins–Olness–Tung (ACOT) ACOT scheme[11] which is based on the renormalization method of Collins–Wilczek–Zee (CWZ).[12] The order-by-order procedure to implement this approach has now been systematically established to all orders in PQCD by Collins.[13]

Recently, additional implementations of VFN schemes have been defined in the literature. While these schemes all agree in principle on the result summed to all orders of perturbation theory, the way of ordering the perturbative expansion is not unique and the results differ at finite order in perturbation theory. The Thorne–Roberts (TR) [14] prescription has been used in the MRST recent global analyses of parton distributions.[15] The BMSN and CNS prescriptions have made use of the $\mathcal{O}(\alpha_s^2)$ calculations by Smith, van Neerven, and collaborators[8, 9] to carry these ideas to higher order. The boundary conditions on the PDF's at the flavor threshold become more complicated at this order; in particular, the PDF's are no longer continuous across the N to N+1 flavor threshold. Buza *et al.*,[8] have computed the matching conditions, and this has been implemented in an evolution program by CSN.[9] More recently, a Simplified-ACOT (SACOT) scheme inspired by the prescription advocated by Collins [13] was introduced;[16] we describe this new scheme in Sec. 4.

3. From Low To High Energy Scale

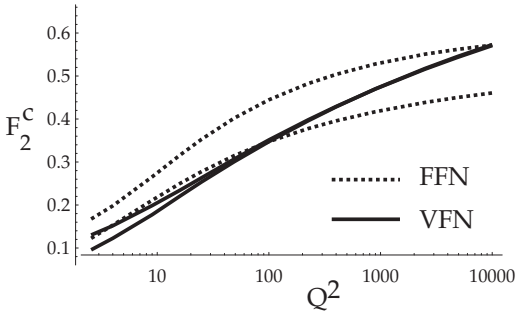

Figure 1. F_2^c for $x = 0.01$ as a function of Q^2 in GeV for two choices of μ as obtained within the $\mathcal{O}(\alpha_s^1)$ FFN and (ACOT) VFN schemes. For details, see Ref. [17].

To compare the features of the FFN scheme with the ACOT VFN scheme[4] concretely, we will take the example of heavy quark production in DIS; the features we extract from this example are directly applicable to the hadroproduction case relevant for the Tevatron Run II. One measure we have of estimating the uncertainty of a calculated quantity is to examine the variation of the renormalization and factorization scale dependence. While this method can only provide a lower bound on the uncertainty, it is a useful tool.

In Fig. 1, we display the component of F_2^c for the $s + W \to c$ sub-process at $x = 0.01$ plotted *vs.* Q^2. We gauge the scale uncertainty by varying μ from $1/2\,\mu_0$to $2.0\,\mu_0$ with $\mu_0 = \sqrt{Q^2 + m_c^2}$. In this figure, both schemes are applied to $\mathcal{O}(\alpha_s^1)$. We observe that the FFN scheme is narrower at low Q, and increases slightly at larger Q. This behavior is reasonable given

[4] In this section we shall use the ACOT VFN scheme for this illustration. The conclusions extracted in comparison to the FFN scheme are largely independent of which VFN scheme are used.

that we expect this scheme to work best in the threshold region, but to decrease in accuracy as the unresummed logs of $\ln^n(Q^2/m_c^2)$ increase.

Conversely, the ACOT VFN scheme has quite the opposite behavior. At low Q, this calculation displays mild scale uncertainty, but at large Q this uncertainty is significantly reduced. This is an indication that the resummation of the $\ln^n(Q^2/m_c^2)$ terms via the heavy quark PDF serves to decrease the scale uncertainty at a given order of perturbation theory. While these general results were to be expected, what is surprising is the magnitude of the scale variation. Even in the threshold region where $Q \sim m_c$ we find that the VFN scheme is comparable or better than the FFN scheme.

At present, the FFN scheme has been calculated to one further order in perturbation theory, $\mathcal{O}(\alpha_s^2)$. While the higher order terms do serve to reduce the scale uncertainty, it is only at the lowest values of Q that the $\mathcal{O}(\alpha_s^2)$ FFN band is smaller than the $\mathcal{O}(\alpha_s^1)$ VFN band. Recently, $\mathcal{O}(\alpha_s^2)$ calculations in the VFN scheme have been performed;[9] it would be interesting to extend such comparisons to these new calculations.

Let us also take this opportunity to clarify a misconception that has occasionally appeared in the literature. The VFN scheme is *not* required to reduce to the FFN scheme at $Q = m_c$. While it is true that the VFN scheme does have the FFN scheme as a limit, this matching depends on the definitions of the PDF's, and the choice of the μ scale.[5] In this particular example, even at $Q = m_c$, the resummed logs in the heavy quark PDF can yield a non-zero contribution which help to stabilize the scale dependence of the VFN scheme result.[6]

The upshot is that even in the threshold region, the resummation of the logarithms via the heavy quark PDF's can help the stability of the theory.

4. Simplified ACOT (SACOT) prescription

We investigate a modification of the ACOT scheme inspired by the prescription advocated by Collins.[13] This prescription has the advantage of being easy to state, and allowing relatively simple calculations. Such simplicity could be crucial for going beyond one loop order in calculations.[7]

> *Simplified ACOT (SACOT) prescription.* Set M_H to zero in the calculation of the hard scattering partonic functions $\widehat{\sigma}$ for incoming heavy quarks.

[5]The general renormalization scheme is laid out in the CWZ paper[12]. The matching of the PDF's at $\mathcal{O}(\alpha_s^1)$ was computed in Ref. [18] and Ref. [19]. The $\mathcal{O}(\alpha_s^2)$ boundary conditions were computed in Ref. [8].

[6] *Cf.*, Ref. [17] for a detailed discussion.

[7]See Ref. [16] for a detailed definition, discussion, and comparisons.

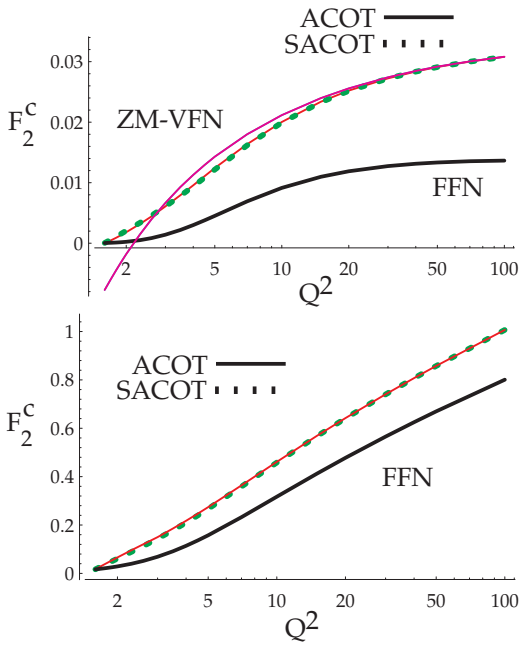

Figure 2. F_2^c as a function of Q^2 in GeV computed to $\mathcal{O}(\alpha_s^1)$ in the ZM-VFN, FFN, ACOT, and SACOT schemes using CTEQ4M PDF's. Fig. a) $x = 0.1$, and Fig. b) $x = 0.001$. Figures taken from Ref. [16].

For example, this scheme tremendously simplifies the calculation of the neutral current structure function F_2^{charm} even at $\mathcal{O}(\alpha_s^1)$. In other prescriptions, the tree process $\gamma + c \to c + g$ and the one loop process $\gamma + c \to c$ must be computed with non-zero charm mass, and this results in a complicated expression.[20] In the SACOT scheme, the charm mass can be set to zero so that the final result for these sub-processes reduces to the very simple massless result.

While the SACOT scheme allows us to simplify the calculation, the obvious question is: does this simplified version contain the full dynamics of the process. To answer this quantitatively, we compare prediction for F_2^{charm} obtained with 1) the SACOT scheme at order α_s^1 with 2) the predictions obtained with the original ACOT scheme, 3) the ZM-VFN procedure in which the charm quark can appear as a parton but has zero mass, and 4) the FFN procedure in which the charm quark has its proper mass but does not appear as a parton. For simplicity, we take $\mu = Q$.

In Fig. 2 we show $F_2^c(x, Q)$ as a function of Q for $x = 0.1$ and $x = 0.001$ using the CTEQ4M parton distributions.[21, 22] We observe that the ACOT and SACOT schemes are effectively identical throughout the kinematic range. There is a slight difference observed in the threshold region, but this is small in comparison

to the renormalization/factorization μ-variation (not shown). Hence the difference between the ACOT and SACOT results is of no physical consequence. The fact that the ACOT and SACOT match extremely well throughout the full kinematic range provides explicit numerical verification that the SACOT scheme fully contains the physics.

Although we have used the example of heavy quark leptoproduction, let us comment briefly on the implications of this scheme for the more complex case of hadroproduction.[1, 23, 24, 25] At present, we have calculations for the all the $\mathcal{O}(\alpha_s^2)$ hadroproduction subprocesses such as $gg \to Q\bar{Q}$ and $gQ \to gQ$. At $\mathcal{O}(\alpha_s^3)$ we have the result for the $gg \to gQ\bar{Q}$ sub-processes, but not the general result for $gQ \to ggQ$ with nonzero heavy quark mass. With the SACOT scheme, we can set the heavy quark mass to zero in the $gQ \to ggQ$ sub-process and thus make use of the simple result already in the literature.[8] This is just one example of how the SACOT has the practical advantage of allowing us to extend our calculations to higher orders in the perturbation theory. We now turn to the case of heavy quark production for hadron colliders.

5. Heavy Quark Hadroproduction

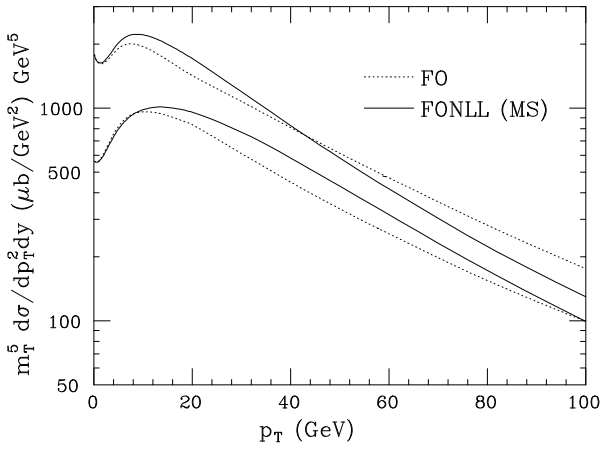

Figure 3. Differential cross section for b-production *vs.* p_T comparing the Fixed-Order (FO) and the Fixed-Order Next-to-Leading-Log (FONLL) result in the $\overline{MS}$ scheme. The bands are obtained by varying independently the renormalization and factorization scales. The cross section is scaled by m_T^5 with $m_T = \sqrt{m_b^2 + p_T^2}$, and $\sqrt{s} = 1800\,GeV$, $m_b = 5\,GeV$, $y = 0$, with CTEQ3M PDF's. Figure taken from Cacciari, Greco, and Nason, Ref. [27].

[8]For a related idea, see the fragmentation function formalism of Cacciari and Greco[26] in the following section.

There has been notable progress in the area of hadroproduction of heavy quarks. The original NLO calculations of the $gg \to b\bar{b}$ subprocess were performed by Nason, Dawson, and Ellis [23], and by Beenakker, Kuijf, van Neerven, Meng, Schuler, and Smith[24]. Recently, Cacciari and Greco[26] have used a NLO fragmentation formalism to resum the heavy quark contributions in the limit of large p_T; the result is a decreased renormalization/factorization scale variation in the large p_T region. The ACOT scheme was applied to the hadroproduction case by Olness, Scalise, and Tung.[25] More recently, the NLO fragmentation formalism of Cacciari and Greco has been merged with the massive FFN calculation of Nason, Dawson, and Ellis by Cacciari, Greco, and Nason,[27]; the result is a calculation which matches the FFN calculation at low p_T, and takes advantage of the NLO fragmentation formalism in the high p_T region, thus yielding good behavior throughout the full p_T range. This is displayed in Fig. 3 where we see that this Fixed-Order Next-to-Leading-Log (FONLL) calculation displays reduced scale variation in the large p_T region, and matches on the the massive NLO calculation in the small p_T region. Further details can be found in the report of the LHC Workshop *b-production group*.[9]

6. W + Heavy Quark Production

PDF Set	Mass (GeV)	LO	WQQ	NLO
CTEQ1M	m_c=1.7	96	20	161
MRSD0'	m_c=1.7	81	20	138
CTEQ3M	m_c=1.7	83	20	141
CTEQ3M	m_b=5.0	0.17	9.09	9.33

Table 1
The W + charm-tagged one-jet inclusive cross section in pb for LO, $W+Q\bar{Q}$, and NLO (including the $W+Q\bar{Q}$ contribution) using different sets of parton distribution functions. Table is taken from Ref. [28].

The precise measurement of W plus heavy quark ($W+Q$) events provides an important information on a variety of issues. Measurement of $W+Q$ allows us to test NLO QCD theory at high scales and investigate questions about resummation and heavy quark PDF's. For example, if sufficient statistics are available, $W+charm$ final states can be used to extract

[9] The LHC Workshop *b-production group* is organized by Paolo Nason, Giovanni Ridolfi, Olivier Schneider, Giuseppe Tartarelli, Vikas Pratibha, and the report is currently in preparation. The webpage for the *b-production group* is located at http://home.cern.ch/n/nason/www/lhc99/

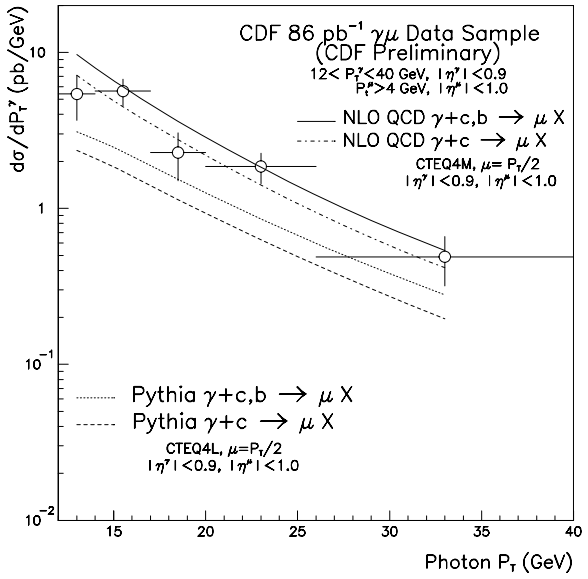

Figure 4. Differential $d\sigma/dp_T^\gamma$ for γ plus tagged heavy quark production as compared with Pythia and the NLO QCD results. Figure taken from Ref. [29].

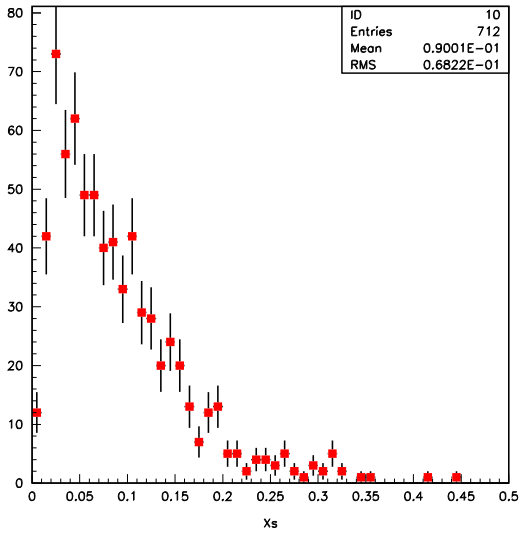

Figure 5. Distribution of $Events/0.01$ *vs.* x of the s-quarks which contribute to the $s + W \to c$ process. Figure taken from Ref. [30].

information about the strange quark distribution. In an analogous manner, the W+*bottom* final states are sensitive to the charm PDF; furthermore, W+*bottom* can fake Higgs events, and are also an important background for sbottom ($\tilde{b}$) searches.

The cross sections for W plus tagged heavy quark jet were computed in Ref. [28], and are shown in Table. 1. Note that this process has a large K-factor, and hence comparison between data and theory will provide discerning test of the NLO QCD theory. While the small cross sections of these channels hindered analysis in Run I, the increased luminosity in Run II can make this a discriminating tool. For example, Run I provided minimal statistics on W+Q, but there was data in the analogous neutral current channel γ+Q. Fig. 4 displays preliminary Tevatron data from Run I and the comparison with both the PYTHIA Monte Carlo and the NLO QCD calculations; again, note the large K-factor. If similar results are attainable in the charged current channel at Run II, this would be revealing.

Extensive analysis the W+Q production channels were performed in Working Group I: "QCD tools for heavy flavors and new physics searches," and we can make use of these results to estimate the precision to which the strange quark distribution can be extracted. We display Fig. 5 (taken from the WGI report[30]) which shows the distribution in x of the s-quarks which contribute to the W+c process.[10] This figure indicates that there will good statistics in an x-range comparable to that investigated by neutrino DIS experiments;[2, 3] hence, comparison with this data should provide an important test of the strange quark sea and the underlying mechanisms for computing such processes.

7. The Strange Quark Distribution

A primary uncertainty for W+*charm* production discussed above comes from the strange sea PDF, $s(x)$, which has been the subject of controversy for sometime now. One possibility is that new analysis of present data will resolve this situation prior to Run II, and provide precise distributions as an input the the Tevatron data analysis. The converse would be that this situation remains unresolved, in which case new data from Run II may help to finally solve this puzzle.

The strange distribution is directly measured by dimuon production in neutrino-nucleon scattering.[11] The basic sub-process is $\nu N \to \mu^- cX$ with a subsequent charm decay $c \to \mu^+ X'$.

The strange distribution can also be extracted indirectly using a combination of charged ($W^\pm$) and neutral (γ) current data; however, the systematic uncertainties involved in this procedure make an accurate determination difficult.[31] The basic idea is to use

[10] For a detailed analysis of this work including selection criteria, see the report of Working Group I: "QCD Tools For Heavy Flavors And New Physics Searches," as well as Ref. [30].

[11] Presently, there are a number of LO analyses, and one NLO analysis.[2, 3]

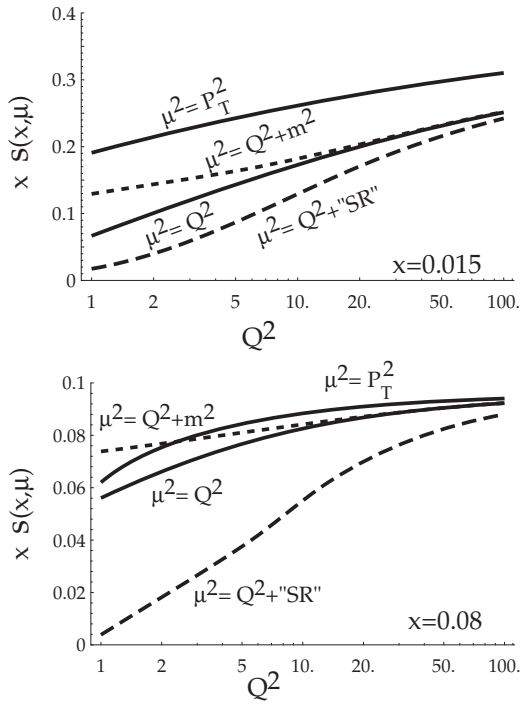

Figure 6. Variation of $x\,s(x,\mu)$ for three choices of μ, and also with a "SR" (slow-rescaling) type correction: $x \to x(1+m_c^2/Q^2)$.

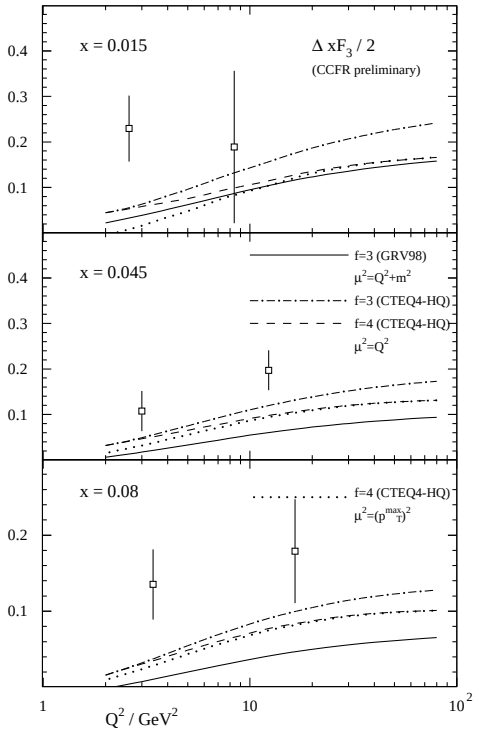

Figure 7. $\Delta xF_3/2$ *vs.* Q^2 for three choices of x. Calculations provided by S. Kretzer.

the relation

$$\frac{F_2^{NC}}{F_2^{CC}} = \frac{5}{18}\left\{1 - \frac{3}{5}\,\frac{(s+\bar{s})-(c+\bar{c})+...}{q+\bar{q}}\right\} \qquad (1)$$

to extract the strange distribution. This method is complicated by a number of issues including the xF_3 component which can play a crucial role in the small-x region—precisely the region where there has been a long-standing discrepancy.

The structure functions are defined in terms of the neutrino-nucleon cross section via:

$$\frac{d^2\sigma^{\nu,\bar{\nu}}}{dx\,dy} = \frac{G_F^2 ME}{\pi}\left[F_2(1-y) + xF_1y^2 \pm xF_3y(1-\frac{y}{2})\right]$$

It is instructive to recall the simple leading-order correspondence between the F's and the PDF's:[12]

$$\begin{aligned} F_2^{(\nu,\bar{\nu})N} &= x\left\{u+\bar{u}+d+\bar{d}+2s+2c\right\} \\ xF_3^{(\nu,\bar{\nu})N} &= x\left\{u-\bar{u}+d-\bar{d}\pm 2s \mp 2c\right\} \end{aligned} \qquad (2)$$

Therefore, the combination ΔxF_3:

$$\Delta xF_3 = xF_3^{\nu N} - xF_3^{\bar{\nu}N} = 4x\{s-c\} \qquad (3)$$

[12] To exhibit the basic structure, the above is taken the limit of 4 quarks, a symmetric sea, and a vanishing Cabibbo angle. Of course, the actual analysis takes into account the full structure.[31]

can be used to probe the strange sea distribution, and to understand heavy quark (charm) production. This information, together with the exclusive dimuon events, may provide a more precise determination of the strange quark sea.

To gauge the dependence of ΔxF_3 upon various factors, we first consider $xs(x,\mu)$ in Fig. 6, and then the full NLO ΔxF_3 in Fig. 7; this allows us to see the connection between ΔxF_3 and $xs(x,\mu)$ beyond leading order. In Fig. 6 we have plotted the quantity $xs(x,\mu)$ *vs.* Q^2 for two choices of x in a range relevant to the the dimuon measurements. We use three choices of the μ^2 scale: $\{Q^2, Q^2+m_c^2, P^2_{T_{max}}\}$. The choices Q^2 and $Q^2+m_c^2$ differ only at lower values of Q^2; the choice $P^2_{T_{max}}$ is comparable to Q^2 and $Q^2+m_c^2$ at $x=0.08$ but lies above for $x=0.015$. The fourth curve labeled Q^2+"SR" uses $\mu^2=Q^2$ with a "slow-rescaling" type of correction which (crudely) includes mass effects by shifting x to $x(1+m_c^2/Q^2)$; note, the result of this correction is significant at large x and low Q^2.

In Fig. 7 we have plotted the quantity $\Delta xF_3/2$ for an isoscalar target computed to order α_s^1. We display three calculations for three different x-bins rele-

vant to strange sea measurement. 1) A 3-flavor calculation using the GRV98[32] distributions,[13] and $\mu = \sqrt{Q^2 + m^2}$. 2) A 3-flavor calculation using the CTEQ4HQ distributions, and $\mu = Q$. 3) A 4-flavor calculation using the CTEQ4HQ distributions, and $\mu = Q$.

The two CTEQ curves show the effect of the charm distribution, and the GRV curve shows the effect of using a different PDF set. Recall that the GRV calculation corresponds to a FFN scheme.

The pair of curves using the CTEQ4HQ distributions nicely illustrates how the charm distribution $c(x, \mu^2)$ evolves as $\ln(Q^2/m_c^2)$ for increasing Q^2; note, $c(x, \mu^2)$ enters with a negative sign so that the 4-flavor result is below the 3-flavor curve. The choice $\mu = Q$ ensures the 3- and 4-flavor calculation coincide at $\mu = Q = m_c$; while this choice is useful for instructive purposes, a more practical choice might be $\mu \sim \sqrt{Q^2 + m^2}$, *cf.*, Sec. 2, and Ref. [17].

For comparison, we also display preliminary data from the CCFR analysis.[31] While there is much freedom in the theoretical calculation, the difference between these calculations and the data at low Q values warrants further investigation.

8. Conclusions and Outlook

A detailed understanding of heavy quark production and heavy quark PDF's at the Tevatron Run II will require analysis of fixed-target and HERA data as well as Run I results. Comprehensive analysis of the combined data set can provide incisive tests of the theoretical methods in an unexplored regime, and enable precise predictions that will facilitate new particle searches in a variety of channels. This document serves as a progress report, and work on these topics will continue in preparation for the Tevatron Run II.

This work is supported by the U.S. Department of Energy, the National Science Foundation, and the Lightner-Sams Foundation.

REFERENCES

1. F. Abe *et al.* [CDF Collaboration], Phys. Rev. Lett. **71**, 2396 (1993); F. Abe *et al.* [CDF Collaboration], Phys. Rev. Lett. **71**, 500 (1993); B. Abbott *et al.* [D0 Collaboration], hep-ex/9907029.
2. J. Yu [CCFR / NuTeV Collaboration], hep-ex/9806030; A. O. Bazarko *et al.* [CCFR Collaboration], Z. Phys. **C65**, 189 (1995); T. Adams *et al.* [NuTeV Collaboration], hep-ex/9906037.
3. P. Vilain *et al.* [CHARM II Collaboration], Eur. Phys. J. **C11**, 19 (1999).
4. J. Breitweg *et al.* [ZEUS Collaboration], Eur. Phys. J. **C12**, 35 (2000); C. Coldewey [H1 and ZEUS Collaborations], Nucl. Phys. Proc. Suppl. **74**, 209 (1999).
5. M. E. Hayes and M. Kramer, J. Phys. G **G25**, 1477 (1999).
6. S. Frixione, M. L. Mangano, P. Nason and G. Ridolfi, hep-ph/9702287. Heavy Flavours II, ed. by A.J. Buras and M. Lindner, World Scientific. pp.609-706.
7. E. Laenen, S. Riemersma, J. Smith, W.L. van Neerven, Nucl. Phys. **B392** (1993) 162; Phys. Rev. **D49** (1994) 5753.
8. M. Buza, Y. Matiounine, J. Smith, R. Migneron, W.L. van Neerven, Nucl. Phys. **B472** (1996) 611; M. Buza, Y. Matiounine, J. Smith, and W. L. van Neerven, Phys. Lett. **B411** (1997) 211; Nucl. Phys. **B500** (1997) 301; Eur. Phys. J. C1, 301,1998.
9. A. Chuvakin, J. Smith, W.L. van Neerven, hep-ph/9910250; hep-ph/0002011; A. Chuvakin, J. Smith, hep-ph/9911504.
10. F.I. Olness, S.T. Riemersma, Phys. Rev. **D51** (1995) 4746.
11. F. Olness, W.K. Tung, Nucl. Phys. **B308** (1988) 813; M. Aivazis, F. Olness, W.K. Tung, Phys. Rev. **D50** (1994) 3085; M. Aivazis, J.C. Collins, F. Olness, W.K. Tung, Phys. Rev. **D50** (1994) 3102.
12. J. Collins, F. Wilczek, and A. Zee, *Phys. Rev.* **D18**, 242 (1978).
13. J.C. Collins, Phys. Rev. **D58** (1998) 094002.
14. R.S. Thorne, R.G. Roberts, Phys. Lett. **B421** (1998) 303; Phys. Rev. **D57** (1998) 6871.
15. A.D. Martin, R.G. Roberts, W.J. Stirling, R.S. Thorne, Eur. Phys. J. C4, 463, 1998.
16. M. Krämer, F. Olness, D. Soper, hep-ph/0003035.
17. C. Schmidt, hep-ph/9706496; J. Amundson, C. Schmidt, W. K. Tung, X. Wang, MSU preprint, in preparation; J. Amundson, F. Olness, C. Schmidt, W. K. Tung, X. Wang, FERMILAB-CONF-98-153-T, Jul 1998.
18. J.C. Collins, W.-K. Tung *Nucl. Phys.* **B278**, 934 (1986).
19. S. Qian, ANL-HEP-PR-84-72; UMI-85-17585.
20. S. Kretzer, I. Schienbein Phys. Rev. **D56** (1997) 1804; Phys. Rev. **D58** (1998) 094035; Phys. Rev. **D59** (1999) 054004.
21. H. L. Lai *et al.*, Phys. Rev. **D55** (1997) 1280; hep-ph/9903282.
22. H. L. Lai and W.-K. Tung, Z. Phys. **C74**, 463 (1997).

[13] The scale choice $\mu = \sqrt{Q^2 + m^2}$ for the 3-flavor GRV calculation precisely cancels the collinear strange quark mass logarithm in the coefficient function thereby making the coefficient function an exact scaling function, *i.e.* independent of μ^2.

23. P. Nason, S. Dawson and R. K. Ellis, Nucl. Phys. **B327**, 49 (1989). P. Nason, S. Dawson and R. K. Ellis, Nucl. Phys. **B303**, 607 (1988).
24. W. Beenakker, W. L. van Neerven, R. Meng, G. A. Schuler and J. Smith, Nucl. Phys. **B351**, 507 (1991). W. Beenakker, H. Kuijf, W. L. van Neerven and J. Smith, Phys. Rev. **D40**, 54 (1989).
25. F. I. Olness, R. J. Scalise and W. Tung, Phys. Rev. **D59**, 014506 (1999)
26. M. Cacciari and M. Greco, Nucl. Phys. **B421**, 530 (1994).
27. M. Cacciari, M. Greco, and P. Nason, hep-ph/9803400, J. High Energy Phys. **05**, 007 (1998).
28. W. T. Giele, S. Keller and E. Laenen, Nucl. Phys. Proc. Suppl. **51C**, 255 (1996); Phys. Lett. **B372**, 141 (1996); hep-ph/9408325.
29. S. Kuhlmann [CDF Collaboration], FERMILAB-CONF-99-165-E, *Prepared for 7th International Workshop on Deep Inelastic Scattering and QCD (DIS 99), Zeuthen, Germany, 19-23 Apr 1999.*
30. R. Demina, J. D. Lykken, K. T. Matchev and A. Nomerotski, hep-ph/9910275.
31. U. K. Yang *et al.* [CCFR-NuTeV Collaboration], hep-ex/9906042.
32. M. Gluck, E. Reya and A. Vogt, Eur. Phys. J. **C5**, 461 (1998).